



You have downloaded a document from
RE-BUŚ
repository of the University of Silesia in Katowice

Title: Isospin Against Size Effects In Projectile Dynamical Fission For $112,124\text{Sn}+58,64\text{Ni}$ and $124\text{Xe}+64\text{Zn}$ Reactions At 35 A.MeV

Author: P. Russotto, E. De Filippo, Andrzej Grzeszczuk, Seweryn Kowalski, Katarzyna Schmidt, Wiktor Zipper i in.

Citation style: Russotto P., De Filippo E., Grzeszczuk Andrzej, Kowalski Seweryn, Schmidt Katarzyna, Zipper Wiktor i in.(2014). Isospin Against Size Effects In Projectile Dynamical Fission For $112,124\text{Sn}+58,64\text{Ni}$ and $124\text{Xe}+64\text{Zn}$ Reactions At 35 A.MeV. "Journal of Physics: Conference Series" (Vol. 515, (2014), art. no. 012020), doi 10.1088/1742-6596/515/1/012020



Uznanie autorstwa - Licencja ta pozwala na kopiowanie, zmienianie, rozprowadzanie, przedstawianie i wykonywanie utworu jedynie pod warunkiem oznaczenia autorstwa.



UNIWERSYTET ŚLĄSKI
W KATOWICACH



Biblioteka
Uniwersytetu Śląskiego



Ministerstwo Nauki
i Szkolnictwa Wyższego

Isospin Against Size Effects In Projectile Dynamical Fission For $^{112,124}\text{Sn} + ^{58,64}\text{Ni}$ and $^{124}\text{Xe} + ^{64}\text{Zn}$ Reactions At 35 A.MeV

P. Russotto¹, E. De Filippo¹, A. Pagano¹, E. Piasecki^{2,3}, L. Acosta⁴, F. Amorini⁴, A. Anzalone⁴, L. Auditore⁵, V. Baran⁶, I. Berceanu⁷, C. Boiano⁸, B. Borderie⁹, M. Bruno¹⁰, T. Cap¹¹, G. Cardella¹, A. Castoldi^{8,12}, S. Cavallaro^{4,13}, M.B. Chatterjee¹⁴, A. Chbihi¹⁵, M. Colonna⁴, M. D'Agostino¹⁰, M. D'Andrea¹, M. Di Toro^{4,13}, F. Fichera¹, L. Francalanza^{4,13}, E. Geraci^{1,13}, R. Gianì^{4,13}, B. Gnoffo¹³, A. Grimaldi¹, A. Grzeszczuk¹⁶, C. Guazzoni^{8,12}, P. Guazzoni^{8,17}, N. Giudice¹, S. Kowalski¹⁶, E. La Guidara¹, G. Lanzalone^{4,18}, G. Lanzaò^{1,23}, I. Lombardo^{19,20}, C. Maiolino⁴, G. Marquín-Durán²¹, T. Minniti¹³, M. Papa¹, E.V. Pagano^{4,13}, G. Passaro⁴, S. Pirrone¹, R. Płaneta²², G. Politi^{1,13}, F. Porto^{4,13}, L. Quattrocchi⁵, M.F. Rivet⁹, E. Rosato^{19,20}, F. Riccio^{8,12}, F. Rizzo^{4,13}, G. Saccà¹, K. Schmidt¹⁶, K. Siwek-Wilczyńska¹¹, I. Skwira-Chalot¹¹, A. Trifirò⁵, M. Trimarchi⁵, G. Verde¹, M. Vigilante^{19,20}, J.P. Wieleczko¹⁵, J. Wilczyński²³, P. Zambon^{8,12}, L. Zetta^{8,17} and W. Zipper¹⁶

¹INFN-Sezione di Catania, Catania, Italy

²Heavy Ion Laboratory, University of Warsaw, Warsaw, Poland

³A. Sołtan Institute for Nuclear Studies, Świerk/Warsaw, Poland

⁴INFN-Laboratori Nazionali del Sud, Catania, Italy

⁵INFN, Gr. Coll. di Messina and Dip. di Fisica e Scienze della Terra, Univ. di Messina, Italy

⁶Physics Faculty, University of Bucharest, Romania

⁷National Institute of Physics and Nuclear Engineering "Horia Hulubei", Bucharest, Romania

⁸INFN, Sezione di Milano, Milano, Italy

⁹Institut de Physique Nucléaire, CNRS/IN2P3, Université Paris-Sud 11, Orsay, France

¹⁰INFN, Sezione di Bologna and Dip. di Fisica, Univ. di Bologna, Italy

¹¹Faculty of Physics, University of Warsaw, Warsaw, Poland

¹²Dip. Eletttronica, Informazione e Bioingegneria, Politecnico di Milano, Milano, Italy

¹³Dip. di Fisica e Astronomia, Univ. di Catania, Catania, Italy

¹⁴Saha Institute of Nuclear Physics, Kolkata, India

¹⁵GANIL (DSM-CEA/CNRS/IN2P3), Caen, France

¹⁶Institute of Physics, University of Silesia, Katowice, Poland

¹⁷Dipartimento di Fisica, Univ. di Milano, Milano, Italy

¹⁸"Kore" Università, Enna, Italy

¹⁹Dip. di Fisica - Univ. di Napoli "Federico II", Compl. Un. Monte S. Angelo ed. 6, Via Cinthia, 80126 Napoli, Italy

²⁰INFN-Sez. di Napoli, Compl. Un. Monte S. Angelo ed. 6, Via Cinthia, 80126 Napoli, Italy

²¹Departamento de Física Aplicada, Universidad de Huelva, E-21071 Huelva, Spain

²²M. Smoluchowski Institute of Physics, Jagellonian Univ., Cracow, Poland

²³deceased



²³National Centre for Nuclear Research, Otwock-Świerk, Poland

E-mail: russotto@lns.infn.it

Abstract. In past experiments, mass asymmetric projectile-target combinations $^{124}\text{Sn}+^{64}\text{Ni}$ and $^{112}\text{Sn}+^{58}\text{Ni}$ were investigated at $E_{Lab}(^{112,124}\text{Sn})=35$ A.MeV beam energy by using the 4π multi-detector CHIMERA. From a quantitative comparison of cross sections associated to Statistical and Dynamical Fission of the Projectile-Like Fragments, it resulted that Dynamical Fission process is about two times more probable in the neutron rich $^{124}\text{Sn}+^{64}\text{Ni}$ system than in the $^{112}\text{Sn}+^{58}\text{Ni}$ neutron poor one. In contrast, no sizable difference was found for Statistical Fission mechanism. The observed difference in the strength of the Dynamical effects could arise from the difference in entrance channel Isospin (N/Z) content. In order to disentangle Isospin effects from effects due to the different masses of the two systems, a new experiment $^{124}\text{Xe}+^{64}\text{Zn}$ at 35 A.MeV beam energy has been recently carried out.

1. Introduction

A characteristic experimental signature of Heavy-Ion reactions in the Fermi energy domain (20-100 A.MeV) is the abundant emission of relatively light fragments, the so called Intermediate Mass Fragments (IMF), having atomic number $Z \geq 3$. IMF show a broad velocity distribution ranging from Target-Like Fragments (TLF) velocity to Projectile-Like Fragments (PLF) one, indicating that their production comes from different reaction mechanisms with characteristic time scales, from dynamical and pre-equilibrium emission to statistical decay of excited systems at equilibrium. In particular, in semi-peripheral reactions, the production of IMF and Light Charged Particles (LCP) in the velocity region between the PLF and TLF (midrapidity) has been experimentally observed and the features of a dynamical origin (not related to a statistical emission from an equilibrated source) have been clearly evidenced in many works (see [1–6] and references therein). In addition, a clear signature of an emission chronology related to the IMF size was demonstrated [1–3, 7, 8]. It was found that lighter IMF ($Z < \sim 9$) in the mid-velocity region are likely to be emitted during the re-separation process of the primary interacting Projectile and Target Like Fragments (PLF* and TLF* respectively) in prompt neck-rupture mechanism (time $< \sim 120$ fm/c) [1, 2, 4, 7]. Many experimental results have shown a net neutron enrichment of fragments in the midvelocity region with respect to the ones coming from the sequential emission of PLF* or TLF* equilibrated nuclei [9–16]. In a recent paper [17] we have proved that the correlation between the isotopic content of the IMF, the alignment properties and the time-scale of their emission can be used to probe the symmetry term of the nuclear Equation of State (EOS) at densities below the saturation one [18].

Conversely, emission of heavier IMF ($Z > \sim 9$) was shown to happen at the late stage of the neck expansion process and was associated with the "Dynamical Fission" mechanism [3, 7, 8, 19, 20]; this is nearly a two-step (sequential) reaction: scattering of primary nuclei (PLF*-TLF*) followed by fast non-equilibrated fission-like process. Our previous analysis [2, 3, 8] suggested that Dynamical Fission occurs in a late stage of the re-separation of the PLF*-TLF* binary system (time > 120 fm/c), but before the PLF* and TLF* have achieved full "equilibration", as it was demonstrated by the experimental anisotropy observed in the angular distribution of the IMF. A very fast (on a time scale of 70-100 fm/c) ternary and quaternary aligned breakup process, following deep inelastic binary reactions, has been also observed in Au+Au collisions at 15A.MeV [21, 22]. However, the reaction mechanism observed in these deep inelastic collisions at lower energies probably differs from that observed at higher energies [3, 6, 8, 20].

In addition to these fast-dynamical mechanisms, much slower equilibrated PLF* and TLF* de-excitation [23], characterized by clear isotropic angular distribution has been observed.

The observed experimental signature of IMF emission supports a time scale evolution of the

reaction, in agreement with predictions of Stochastic Mean Field (SMF) [24, 25] and molecular dynamics (CoMD-II) [7] calculations.

In [8] cross sections associated to Dynamical and Statistical Fission mechanisms for neutron rich $^{124}\text{Sn}+^{64}\text{Ni}$ and neutron poor $^{112}\text{Sn}+^{58}\text{Ni}$ reactions at 35 A.MeV beam energy (REVERSE experiment) were evaluated. It was shown that Dynamical Fission process is about two times more probable in the neutron rich $^{124}\text{Sn}+^{64}\text{Ni}$ system than in the $^{112}\text{Sn}+^{58}\text{Ni}$ neutron poor one. This sizable difference in the cross section associated to Dynamical Fission indicates a strong influence of the entrance channel on the reaction mechanism. However, in order to disentangle Isospin effects from effects due to the different size of the two systems, a new experiment (InKiIsSy) with system $^{124}\text{Xe}+^{64}\text{Zn}$ at 35 A.MeV beam energy has been recently carried out.

In section 2 we briefly review the previous results of the REVERSE experiment, already published in refs. [3, 8], that constitute the motivations of the new InKiIsSy experiment, that will be briefly presented in section 3.

2. Previous experimental results and motivations of the InKiIsSy experiment

The REVERSE experiment was performed at the INFN-LNS Super-Conducting Cyclotron of Catania (Italy), bombarding thin ($\approx 300\mu\text{g}/\text{cm}^2$) self-supporting ^{64}Ni and ^{58}Ni targets with 35 A.MeV ^{124}Sn and ^{112}Sn beams, respectively. Reaction products were detected with the forward part of the 4π multi-detector CHIMERA [1] that is constituted by 688 Si($\approx 300\mu\text{m}$)-CsI(Tl) telescopes over a total of 1192, arranged in 18 rings and covering the angular range between 1° and 30° . Further information about CHIMERA multi-detector and REVERSE experiment can be found in [26]. Details about the experimental methods can be found in our previous works [1–3, 27] and refs. therein.

In order to select peripheral collisions, the method of Cavata [28] was used to estimate the impact parameter from the total charged-particle multiplicity. This method assumes a purely geometrical monotonic correlation between the total charged-particle multiplicity of the collision process and the impact parameter. Fig. 1 shows the correlation between the experimental total charged particles multiplicity and the estimated reduced impact parameter $b_{red} = b/b_{Max}$ for the two reactions $^{124}\text{Sn}+^{64}\text{Ni}$ and $^{112}\text{Sn}+^{58}\text{Ni}$ at 35 A.MeV, where b_{Max} corresponds to the total geometrical cross section. Note that at a fixed b_{red} the neutron poor system produces a higher (by \approx one unit) multiplicity. In fact, as predicted by calculations [10, 25], in the neutron poor system the dynamical and pre-equilibrium phases lead to more light charged particles (mainly protons) emission than in neutron rich one where, in contrast, neutron emission is favored.

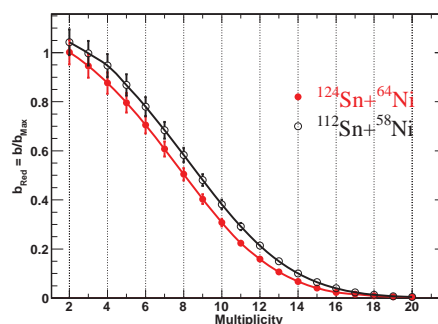


Figure 1. Estimated reduced impact parameter b_{red} plotted as function of the experimental total charged particles multiplicity for the $^{124}\text{Sn}+^{64}\text{Ni}$ and $^{112}\text{Sn}+^{58}\text{Ni}$ reactions at 35 A.MeV, as obtained by applying the method of Cavata [28].

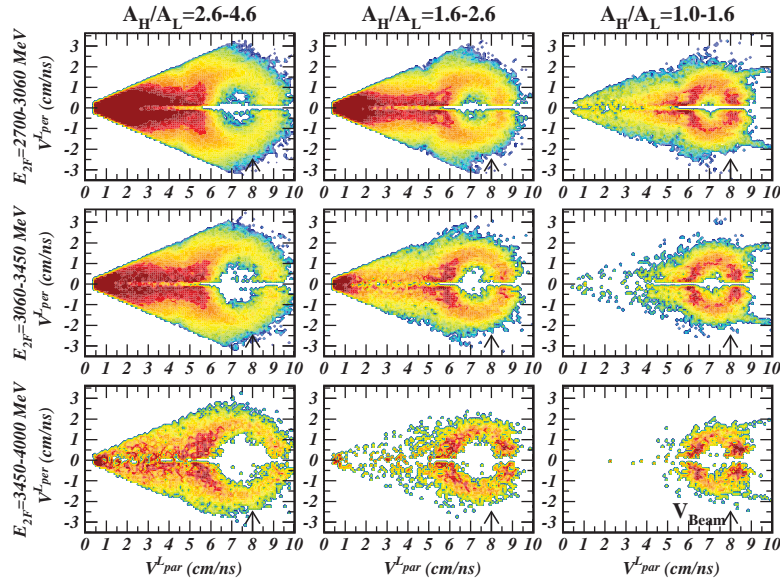


Figure 2. Invariant V_{par} versus V_{per} plots for the Light fragments in the $^{124}\text{Sn}+^{64}\text{Ni}$ reaction at 35 A.MeV. Different panels correspond to different values of mass asymmetry A_H/A_L and total kinetic energy $E_{2F} = E_H + E_L$. The distributions are shown in logarithmic scale. The red color corresponds to the largest cross sections and the arrows indicate the beam velocity.

After selecting, in both systems, peripheral collisions with condition $b_{red} > 0.7$, the two heaviest fragments of the chosen subset of events, named as Heavy (H) and Light (L) according to their atomic number Z , were analyzed in those events that satisfy the following conditions: (i) the combined charge of the two selected fragments $Z_{2F} = Z_H + Z_L$ is close to the charge of the projectile ($Z_{proj} = 50$), that is, $37 < Z_{2F} < 57$, and (ii) the Heavy-to-Light-fragment mass ratio is $A_H/A_L < 4.6$, so that the Light fragment has charge $Z_L > \sim 9$. Applying such conditions, the Heavy fragments have the component of the velocity parallel to the beam axis (V_{par}^H) very close to the value of ~ 7.5 cm/ns, that is, slightly below the beam velocity of ~ 8 cm/ns, while the Light fragments have a wider distribution of the parallel velocity, ranging from the velocity of the TLF (~ 1 cm/ns) up to velocities exceeding the PLF ones. This is shown in Fig. 2, where, using a logarithmic intensity scale, the V_{par} versus V_{per} Galilean-invariant plots for Light fragments produced in the $^{124}\text{Sn}+^{64}\text{Ni}$ reaction are presented, for three ranges of mass asymmetry A_H/A_L (columns), and for three ranges of the total kinetic energy of the two selected fragments $E_{2F} = E_H + E_L$ (rows). The quantity E_{2F} is a measure of the collision violence: larger values of E_{2F} are associated with more gentle (peripheral) collisions, while more violent collisions are associated with smaller E_{2F} values. In all panels of Fig. 2 it is possible to observe the characteristic Coulomb rings centered slightly below the beam velocity; the presence of such rings points to PLF* as a well-defined decay source and proves the scenario of two separate reaction steps: first the scattering of the PLF*, followed by its splitting into two fragments (H and L). In almost symmetric divisions after less dissipative collisions [$E_{2F}=3450-4000$ MeV and $A_H/A_L = 1.0-1.6$], the Light fragments distribution is forward-backward symmetric, that is, the Light fragments have equal probability to be emitted forward or backward in the reference frame of the PLF* source. This result is characteristic of an equilibrated fission, where the nucleus is supposed to be completely equilibrated in all its degrees of freedom; there, the PLF* splitting is expected to occur a long time (1000 fm/c or more) after at least one complete rotation. In more

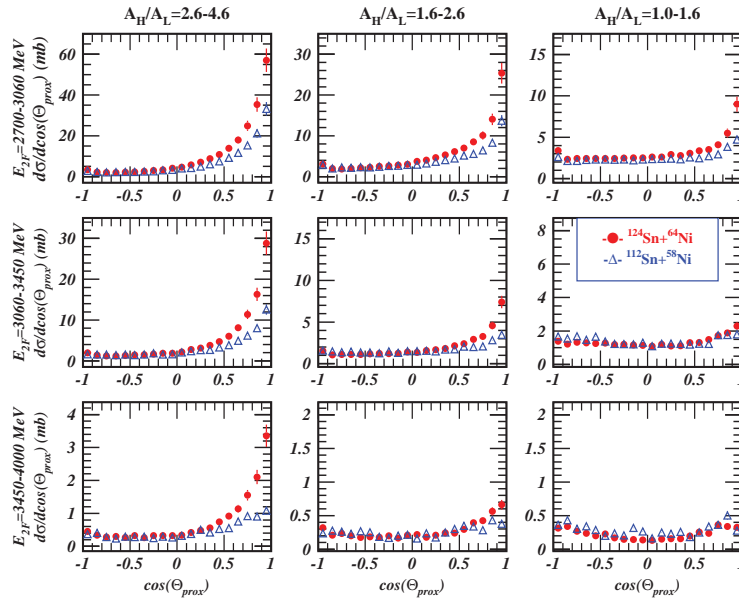


Figure 3. $\cos(\theta_{prox})$ angular distributions of the PLF break-up fragments for the $^{124}\text{Sn}+^{64}\text{Ni}$ (circles) and $^{112}\text{Sn}+^{58}\text{Ni}$ (triangles) at 35 A.MeV, for three different bins of the total kinetic energy (E_{2F}) and mass asymmetry A_H/A_L .

dissipative collisions and/or more asymmetric splits, the population of the Coulomb ring is no longer forward-backward symmetric. In fact, Light fragments have the tendency to populate preferentially the low-velocity side of the Coulomb ring, which means that they are backward-emitted in the PLF* reference frame, that is, toward the TLF*. Nonetheless, a forward-backward symmetric component is still present. Therefore, the observed distributions can be interpreted as a superposition of a forward-backward symmetric component and an asymmetric one. The observed forward-backward asymmetry is the main signature of the Dynamical Fission; that indicates that PLF* fission-like splitting has to be a fast process.

After selecting Light fragments populating the Coulomb ring by gating on V_{par}^L (see ref. [3] for details), in order to disentangle and estimate isotropic and anisotropic fission-like splitting in the two Sn+Ni systems, the differential cross sections $d\sigma/d\cos(\theta_{prox})$ have been evaluated. That is shown in Fig. 3 for the three bins of the mass asymmetry A_H/A_L and three bins of the E_{2F} . The θ_{prox} , defined in left panel of Fig. 4, is the angle between the PLF* flight direction (in the CM reference frame) before fission-like splitting, and the breakup axis, defined by the relative velocity of the two fission-like fragments $\mathbf{V}^H - \mathbf{V}^L$. The value of $\cos(\theta_{prox}) = 1$ corresponds to the Heavy fragment moving forward along the PLF* flight direction, while the Light fragment is emitted backward along the PLF*-TLF* direction. In the case of equilibrated splitting, a symmetric distribution around the value of $\cos(\theta_{prox}) = 0$ is expected, as observed in Fig. 3 for almost symmetric splitting in more peripheral collisions. Instead, by progressively increasing the mass asymmetry and inelasticity (lower E_{2F}), an increase of a forward peaked distribution, superimposed to a symmetric one around the value of $\cos(\theta_{prox}) = 0$, is clearly seen; that is associated to the Dynamical Fission. In order to isolate the equilibrated component, a symmetrization around $\cos(\theta_{prox}) = 0$ of the backward part, $\cos(\theta_{prox}) < 0$, of the distribution has been done, by assuming that the latter is not influenced by Dynamical Fission. The Dynamical contribution is then obtained by subtracting the extrapolated Statistical Fission distribution from the total experimental one. A sketch of this procedure is shown in the right

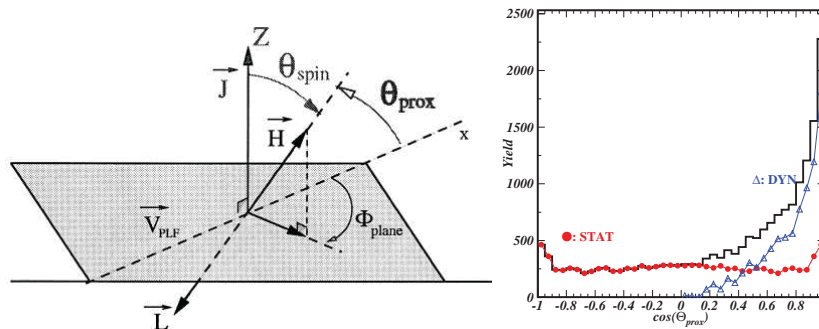


Figure 4. left panel: θ_{prox} definition: angle between the breakup axis, oriented from the light L to the heavy fragment H, and the recoil velocity in the center of mass of the projectile-like fragment (noted V_{PLF}) reconstructed with the two fission fragments, from [20]; right panel: example of extrapolation of Dynamical and Statistical Fission from $\cos(\theta_{prox})$ distribution.

panel of Fig. 4. It results that the Statistical Fission cross section is approximately the same in the two systems. In contrast the Dynamical component is larger for the neutron rich system by a factor of about 2 as compared with the neutron poor one, as can be found in tables published in ref. [8]. This sizable difference in the cross section associated to Dynamical Fission indicates a strong influence of the entrance channel on the reaction mechanism. Since the two systems have a large difference in the Isospin content (see table 1) it appears quite natural to link this to an Isospin effect; however, a possible influence of the system size can not be a priori excluded.

3. The InKiIsSy experiment

In order to disentangle entrance channel Isospin effects from the possible dependence of these results upon the initial different mass of the two systems, in April 2013 we carried out a new experiment, named InKiIsSy (Inverse Kinematic Isobaric Systems) [29], using a projectile/target combination having the same mass as the neutron rich $^{124}\text{Sn} + ^{64}\text{Ni}$ system and a N/Z near to value of the neutron poor $^{112}\text{Sn} + ^{58}\text{Ni}$ one, that is $^{124}\text{Xe} + ^{64}\text{Zn}$ at the same bombarding energy of 35 A.MeV; Isospins of investigated systems are given in table 1. The experiment has been

Table 1. Isospin (N/Z) of the systems investigated in the REVERSE and InKiIsSy experiments

<i>System</i>	<i>N/Z Projectile</i>	<i>N/Z Target</i>	<i>N/Z Compound</i>
$^{124}\text{Sn} + ^{64}\text{Ni}$	1.48	1.29	1.41
$^{112}\text{Sn} + ^{58}\text{Ni}$	1.24	1.07	1.18
$^{124}\text{Xe} + ^{64}\text{Zn}$	1.30	1.13	1.24

performed at the INFN-LNS in Catania by using the 4π CHIMERA multi-detector. By using CHIMERA we will provide new data set to be compared to the old one. Besides, CHIMERA was coupled to 4 prototypes of the new correlator FARCOS (Femtoscope Array for CORrelation and Spectroscopy) [30]. The FARCOS detector has been designed as a compact high resolution array; it is composed of telescopes, each one made of two double-sided silicon-strip detectors (DSSSD) of $64 \times 64 \text{ mm}^2$ area and thickness of 300 and 1500 μm , respectively, facing the target,

followed by 4 CsI(Tl) crystals of $32 \times 32 \times 60 \text{ mm}^3$. The light produced by each crystal is read-out by a Photo-Diode with a thickness of $300 \text{ }\mu\text{m}$ and an active area of $2.5 \times 2.5 \text{ cm}^2$.

Concerning the silicon strip detectors, each DSSSD is segmented in 32 horizontal and 32 vertical strips, from which it is possible to define 1024 individual pixels each covering an area of $2 \times 2 \text{ mm}^2$. A schematic drawing of the different stages of one FARCOS telescope is shown in upper panel of Fig. 5. In the InKiIsSy experiment, we used four telescopes placed at 25 cm from the target, covering the laboratory polar angles $\theta_{lab} \approx 15^\circ - 45^\circ$, and azimuthal interval $\Delta\phi_{lab} \approx 90^\circ$. In this angular region we will, however, detect LCP and IMF with a higher angular resolution. In addition, there we can measure with high relative momentum resolution p-p and fragment-fragment correlations, with an accurate event characterization (centrality, reaction mechanism,...) based on fragments detected in coincidence by CHIMERA. In fact one of the observable that has recently been suggested to be sensitive to the density dependence of the symmetry energy is represented by nucleon-nucleon correlation function [31, 32]. In particular it is expected that space-time properties of fast proton emitting sources in central collisions between N/Z-asymmetric nuclei depend on the stiffness of the symmetry energy, affecting proton and neutron emission times. The N/Z dependence of two-proton correlations has been recently investigated in $^{40}\text{Ca} + ^{40}\text{Ca}$ vs $^{48}\text{Ca} + ^{48}\text{Ca}$ collisions at beam energy of 80 A.MeV [33].

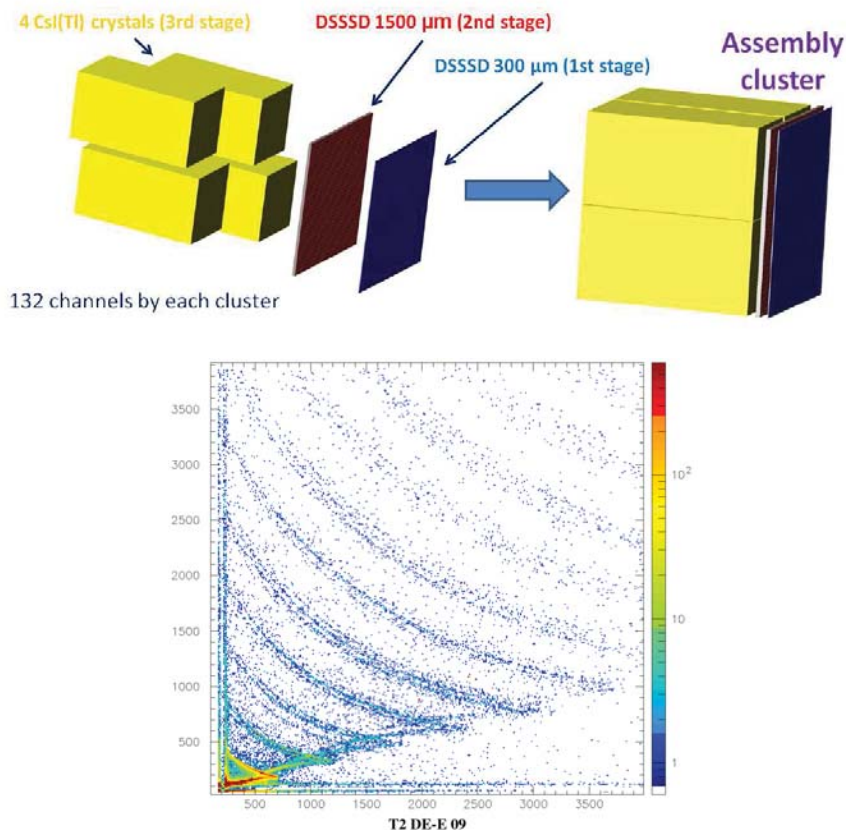


Figure 5. Upper panel: Structure of a FARCOS telescope. The two double-sided silicon strip detectors are followed by 4 CsI(Tl) crystals in a 2 rows x2 columns configuration. Lower panel: $\Delta E(\text{Si } 300 \text{ }\mu\text{m}) - E(\text{Si } 1500 \text{ }\mu\text{m})$ scatter plot for a couple of strips as obtained by a FARCOS telescope prototype in the InKiIsSy experiment.

However, two-proton correlations are also sensitive to the size of the emitting system; thus, it is difficult to attribute the observed N/Z-effect to an Isospin phenomenon rather than to a system size effect. The InKiIsSy experiment may provide a first set of data to characterize FARCOS performance, study emission of LCP and IMF with high resolution and test feasibility of correlation measurements. Effective correlation measurements require, especially considering the demands in terms of statistics, dedicated experiments that we plan to perform in the future. As an example of FARCOS response, lower panel of Fig. 5 shows a $\Delta E(\text{Si } 300 \mu\text{m})$ - $E(\text{Si } 1500 \mu\text{m})$ scatter plot for a couple of strips as obtained during the InKiIsSy experiment; a clear isotope identification is visible. Data analysis is in progress.

From theoretical side, the Dynamical Fission phenomenon has been studied by transport model simulations. The Stochastic Mean Field simulation (SMF) [24] is a good approach in order to describe the gross features of Dynamical Fission. However, the simulation can hardly follow the complete time evolution of the deformed PLF up to the scission point. Many features of the Dynamical Fission processes could be reproduced in quantum molecular dynamics models like the Constrained Molecular Dynamics (CoMD-II) [7]. The main feature of this last model is a self-consistent N -body approach that solves the equations of motion using procedures to satisfy event-by-event the Pauli principle and the total angular momentum conservation law. Then, we plan to perform future studies using both SMF and CoMD-II models in order to shed light on the observations here reported.

References

- [1] A. Pagano *et al.*, Nucl. Phys. A **734**, 504 (2004).
- [2] E. De Filippo *et al.*, Phys. Rev. C **71**, 044602 (2005).
- [3] E. De Filippo *et al.*, Phys. Rev. C **71**, 064604 (2005).
- [4] M. Di Toro *et al.*, Eur. Phys. J. A **30**, 65 (2006).
- [5] S. Piantelli *et al.*, Phys. Rev. C **76**, 061601 (2007).
- [6] A.B. McIntosh *et al.*, Phys. Rev. C **81**, 034603 (2010).
- [7] M. Papa *et al.*, Phys. Rev. C **75**, 054616 (2007).
- [8] P. Russotto *et al.*, Phys. Rev. C **81** 064605 (2010).
- [9] Z. Kohley *et al.*, Phys. Rev. C **83**, 044601 (2011).
- [10] R. Planeta *et al.*, Phys. Rev. C **77**, 014610 (2008).
- [11] S. Piantelli *et al.*, Phys. Rev. C **74**, 034609 (2006).
- [12] J. Lukasik *et al.*, Phys. Rev. C **55**, 1906 (1997).
- [13] D.V. Shetty *et al.*, Phys. Rev. C **68**, 054605 (2003).
- [14] D. Theriault *et al.*, Phys. Rev. C **74**, 051602(R) (2006).
- [15] S. Hudan *et al.*, Phys. Rev. C **86**, 021603(R) (2012).
- [16] S. Barlini *et al.*, Phys. Rev. C **87**, 054607 (2013).
- [17] E. De Filippo *et al.*, Phys. Rev. C **86**, 014610 (2012).
- [18] M.B. Tsang *et al.*, Phys. Rev. C **86**, 015803 (2012).
- [19] A.A. Stefanini *et al.*, Z. Phys. A **351**, 167 (1995).
- [20] F. Bocage *et al.*, Nucl. Phys. A **676**, 391 (2000). 067604 (2010).
- [21] I. Skwira-Chalot *et al.*, Phys. Rev. Lett. **101**, 262701 (2008).
- [22] J. Wilczyński *et al.*, Phys. Rev. C **81**, 024605 (2010) and Phys. Rev. C **81**, 067604 (2010).
- [23] R.J. Charity *et al.*, Phys. Rev. C **82**, 014610 (2010).
- [24] V. Baran, M. Colonna and M. Di Toro, Nucl. Phys. A **730**, 329 (2004).
- [25] V. Baran, M. Colonna, V. Greco, M. Di Toro, Phys. Rep. **410**, 335 (2005).
- [26] A. Pagano *et al.*, Nucl. Phys. A **681**, 331 (2001).
- [27] E. Geraci *et al.*, Nucl. Phys. A **732**, 173 (2004).
- [28] C. Cavata *et al.*, Phys. Rev. C **42**, 1760 (1990).
- [29] P. Russotto, E. De Filippo, A. Pagano and the EXOCHIM collaboration, InKiIsSy Experiment approved by the INFN-LNS PAC 2012.
- [30] G. Verde *et al.*, Jour. of Phys. Conf. Series **420**, 012158 (2013).
- [31] L.W. Chen *et al.*, Phys. Rev. C **68**, 014605 (2004).
- [32] G. Verde, A. Chbihi, R. Ghetti and J. Helgesson, Eur. Phys. J. A **30**, 81 (2006).
- [33] V. Henzl *et al.*, Phys. Rev. C **85**, 014606 (2012).